*Journal of the European Ceramic Society* 17 (1997) 1819–1824

PII: S0955-2219(97)00063-0
0955-2219/97/$17.00 + 0.00

# $Ti_xTa_{1-x}(O,N)_y$ Phases formed by Ammonolysis of Ti–Ta Gels: Preparation of an Anatase-type Solid Solution Phase $Ti_xTa_{1-x}O_{1+x}N_{1-x}$, $0.52 \leq x \leq 0.87$

J. Grins

Department of Inorganic Chemistry, Arrhenius Laboratory, Stockholm University, S-106 91 Stockholm, Sweden

***Abstract***

*Phase formation in the system $Ti_xTa_{1-x}(O,N)_y$ has been studied by ammonolysis of Ti–Ta gels prepared by the sol–gel technique, at temperatures between 600 and 1000°C. The observed phases were characterised by X-ray powder diffraction (XRPD), scanning electron microscopy (SEM) and thermogravimetric (TG) analysis. A monophasic oxynitride with composition $Ti_xTa_{1-x}O_{1+x}N_{1-x}$ and with the anatase type structure was prepared at 600–650°C for $0.52 \leq x \leq 0.87$. The structure was verified for the composition $Ti_{0.68}Ta_{0.32}O_{1.68}N_{0.32}$ ($x = 0.68$) by the Rietveld method ($R_F = 3.0\%$) using CuK$\alpha_1$ XRPD data. Electric conductivity and magnetic susceptibility measurements showed semiconductor and temperature-independent paramagnetic behaviour, respectively. A NaCl-type phase was obtained for $0.52 \leq x \leq 1$ at 900–1000°C. Its unit-cell volume varied both with metal composition and preparation temperature. $Ta_4N_5$- and $Ta_5N_6$-type phases were obtained for $x \leq 0.34$ at 1000°C. Their unit-cell volumes decreased with increasing x, implying that Ti is incorporated in the two types of structures.* © *1997 Elsevier Science Limited.*

## 1 Introduction

The present work is part of a programme the aim of which is to synthesise and characterise new transition metal (oxy)nitrides. In a previous investigation, phase formation in the $Zr_xTa_{1-x}(O,N)_y$ system was studied by ammonolysis of Zr–Ta gels.[1] It was found that a solid-solution phase $Zr_xTa_{1-x}O_{1+x}N_{1-x}$, $0 \leq x \leq 1$, isotypic with the monoclinic modification of $ZrO_2$ structure, can be prepared at 800°C. The present work consists of a similar study of phases formed in the $Ti_xTa_{1-x}(O,N)_y$ system upon ammonolysing homogeneous gels containing Ti and Ta.

The known (oxy)nitrides of Ta, with Ta in high oxidation states, include TaON, $Ta_3N_5$, $Ta_4N_5$ and $Ta_5N_6$.[1] Most of the known Ti (oxy)nitrides are confined to compositions $TiN_n$ with $n \leq 1$.[2] Phases isotypic with $Ti_nO_{2n-1}$ ($n = 2$, 3 and 5) have, however, been obtained by heat treatment of mixtures of $TiO_2$ and TiN in argon atmosphere.[3] No Ti–Ta oxynitrides containing both $Ti^{4+}$ and $Ta^{5+}$ ions have been reported so far.

## 2 Experimental

The materials ammonolysed were gels containing Ti and Ta, with metal compositions of 15, 25, 34, 52, 68, 76, 87 and 100 at% Ti. The gels were prepared by dissolving $TaCl_5$ (Aldrich) and Ti-isopropoxide (Aldrich) in dry ethanol. The clear solution was stirred for 10 min and then hydrolysed by rapid injection of water. The amount of water corresponded to twice the amount of alkoxide present. Hydrolysis was carried out under neutral conditions by adding $NH_3$ to the water, in an amount equivalent to the HCl formed by the dissolution of $TaCl_5$. Xerogels were then obtained by evaporation of the solvent on a hot-plate. The gels were placed in small alumina crucibles and heat-treated in flowing $NH_3$ gas at temperatures between 600 and 1000°C. An $NH_3$ gas flow of 1–2 ml $s^{-1}$ was used, and the ammonolyses were ended by cooling the samples within the furnace to *ca* 100°C.

A JEOL JSM-820 scanning electron microscope (SEM) with an energy-dispersive X-ray (EDX) microanalysis system LINK AN 10000 was used to

characterise the products. Metal compositions were determined by averaging 20 EDX point analyses. The statistical error in each EDX analysis was *ca* 1 at%.

The synthesised materials were characterised by their X-ray powder diffraction (XRPD) patterns, recorded with a Guinier-Hägg camera, using CuK$\alpha_1$ radiation and Si as an internal standard. The patterns were evaluated with a film-scanning system. The relative proportions of the phases present were visually estimated from reflection intensity ratios. XRPD data for Rietveld refinements were collected on a STOE STADI-P diffractometer, using CuK$\alpha_1$ radiation, a rotating sample in transmission mode and a linear position-sensitive detector covering 4·6° in 2$\theta$. A local version of the DBW3·2S full-profile refinement program[4] was used for the structure refinements.

TG recordings were obtained with a Perkin-Elmer TGS-2 TG analyser, operated in air with a heating rate of 10°C min$^{-1}$.

Magnetic measurements were carried out in a weak field ac-susceptometer (Lake Shore 7130) in the temperature range 11–320 K, using a magnetic field of 500 A m$^{-1}$ and a frequency of 707 Hz.

## 3 Results

SEM images showed the gels to consist of fragments, resembling crystallites, with a variation in size from 100 $\mu$m down to less than 0·1 $\mu$m. The nominal metal compositions were checked by EDX and found to be correct within 2 at%. No metal inhomogenities could be discerned and the standard deviations of the EDX point analyses averaged 1·1 at%. The gels contained varying amounts of Cl, up to 20 at% relative to the metal content, originating from the $TaCl_5$ precursor. The ammonolysed gels showed SEM images similar to those of the xero-gels, with the difference that the larger gel fragments were broken up and perforated. No metal segregation could be observed by EDX in the ammonolysed samples, including those found to consist of more than one phase by XRPD. This indicates either that the coexisting phases have essentially the same metal compositions, or that their spatial dimensions are considerably smaller than the dimension sampled in the analysis, *ca* 0·5 $\mu$m. The analyses showed no signal from possible residual Cl.

Guinier-Hägg powder patterns of the ammonolysed gels showed that, under the experimental conditions employed, six different types of phases were formed: (i) phases isotypic with the (oxy)nitrides TaON, $Ta_3N_5$, $Ta_4N_5$, $Ta_5N_6$;[1,5] (ii) a phase isotypic with anatase ($TiO_2$);[6,7] and (iii) cubic NaCl-type phases with a nominal formula $(Ta,Ti)(O,N)_y$. The XRPD patterns of the phases generally exhibited broad Bragg peaks. Figure 1 shows the phases, and their estimated relative amounts, observed at different preparation temperatures and Ti:Ta ratios. The results for preparations containing only Ta (x = 0) are from [1].

### 3.1 Phases isotypic with TaON, $Ta_3N_5$, $Ta_4N_5$ and $Ta_5N_6$

A phase isotypic with monoclinic TaON was observed only in one Ti-containing sample, x = 0·15 prepared at 800°C, together with a $Ta_3N_5$-type phase. Its unit–cell volume 127·2 Å$^3$ is only marginally smaller than that observed for TaON,[8] 127·8 Å,$^3$ and thus it cannot be concluded whether the phase contains Ti.

An orthorhombic $Ta_3N_5$-type[9] phase was obtained in preparations at 650 to 900°C. At 650°C it was obtained X-ray pure for x = 0·15 and together with the anatase-type phase for $0{\cdot}25 \leq x \leq 0{\cdot}34$. Similar results were obtained at 700°C. At 800 and 900°C it was found together with the cubic phase for $0{\cdot}25 \leq x \leq 0{\cdot}68$ and $0{\cdot}15 \leq x \leq 0{\cdot}34$, respectively. The observed unit–cell parameters for the X-ray pure sample (x = 0·15, prepared at 700°C, $a = 3{\cdot}898(1)$, $b = 10{\cdot}128(2)$, $c = 10{\cdot}218(2)$ Å, $V = 403{\cdot}4$ Å$^3$), are significantly different from those of $Ta_3N_5$[1] (prepared at 900°C), $a = 3{\cdot}8900(4)$, $b = 10{\cdot}224(1)$, $c = 10{\cdot}273(1)$ Å, $V = 408{\cdot}6$ Å,$^3$ indicating that at least 15% Ti can be incorporated into $Ta_3N_5$. The unit–cell volumes for the $Ta_3N_5$-type phase in the multi-phase materials with $x \geq 0{\cdot}15$ showed a further decrease with increasing overall Ti content, down to *ca* 400 Å,$^3$ suggesting that these phases may contain still higher amounts of Ti. The variation of the unit–cell volumes was not systematic, however, and showed a general increase of unit–cell volumes with preparation temperature. Previous studies have shown that

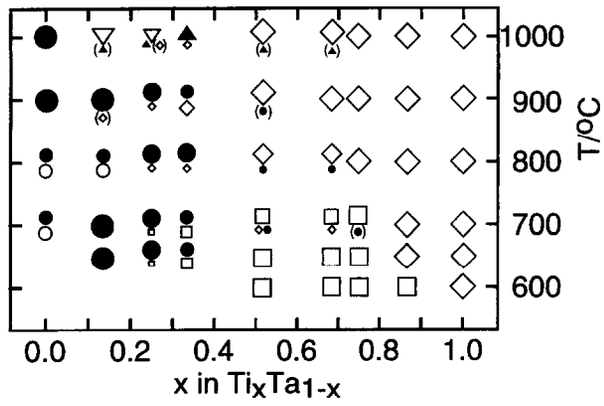


**Fig. 1.** An illustration of observed phases at different preparation temperatures. Estimated relative amounts of the phases are indicated by the sizes of the symbols. Symbols in parentheses indicate traces. (●), $Ta_3N_5$; (▽), $Ta_4N_5$; (▲), $Ta_5N_6$; (○), TaON; (◇), cubic NaCl-type; (□), anatase.

$Ta_3N_5$-type phases may contain anion vacancies (e.g. in $Ta_3N_{4.66(2)}$),[5] as well as cation vacancies (e.g. in $Ta_{2.20}Nb_{0.34}N_{3.92}O_{1.08}$).[5] The present observations may thus be taken to indicate non-stoichiometries in the $Ta_3N_5$-type phases in accord with previous reports.

Phases isotypic with $Ta_4N_5$ (possessing an NaCl-related tetragonal structure with $a = 6.842(2)$ and $c = 4.266(4)$ Å, $V = 199.7$ Å$^3$ and $Ta_5N_6$ (possessing a hexagonal structure with $a = 5.178(1)$ and $c = 10.346(6)$ Å, $V = 240.3$ Å$^3$ were obtained at 1000°C. The sample with $x = 0.15$ contained $Ta_4N_5$-type with a minor amount of $Ta_5N_6$-type, the sample with $x = 0.25$ additional the cubic phase, and the sample with $x = 0.34$ a mixture of the $Ta_5N_6$-type and the cubic phase. The derived unit-cell volumes for the phases are shown in Fig. 2 together with the unit-cell volumes for $Ta_4N_5$ and $Ta_5N_6$.[1] Both phases show a linear decrease in cell volume with increasing x which indicates that they both can incorporate substantial amounts of Ti.

### 3.2 Anatase-type $Ti_xTa_{1-x}O_{1+x}N_{1-x}$, $0.52 \leq x \leq 0.87$.

An anatase-type phase was observed at 600–700°C. Its powder pattern could be indexed with a body-centered tetragonal unit cell, with $a = 3.8$–$3.9$ Å and $c = 9.5$–$10.0$ Å. It was obtained X-ray pure for $0.52 \leq x \leq 0.87$ at 600°C and for $0.52 \leq x \leq 0.76$ at 650°C. The colour of the phase was dark green. At lower x values it was found coexisting with a $Ta_3N_5$-type phase and at higher x-values with a NaCl-type phase, the amounts of these secondary phases increasing with preparation temperature. At 600°C, the samples with $x \leq 0.25$ were X-ray amorphous and the sample with $x = 0.34$ showed only one weak and broad line from the anatase phase.

The derived unit-cell volumes for the anatase-type phase $Ti_xTa_{1-x}O_{1+x}N_{1-x}$ are shown in Fig. 3, together with the unit-cell volume for the anatase modification of $TiO_2$.[6] A linear decrease in cell volume from 151.5 Å$^3$ to 136.3 Å,$^3$ *ca* 10%, is observed when going from $x = 0.25$ to $x = 1$. Such a decrease is in agreement with the replacement of $Ta^{5+}$ ions by smaller $Ti^{4+}$ ions. The *a* and *c* axes were thus found to decrease in a linear manner with the Ti content. The c–a ratios were similar to that of anatase, 2.52, varying between 2.51 and 2.55. It should be noted that the data given in Fig. 3 originates from multi- as well as mono-phasic samples The observed linear variation of the unit-cell volume with x thus suggests that the occurrence of the anatase phase together with the other phases does not involve metal segregation, as no evidence of metal inhomogeneities was revealed by the EDX studies. TG heating runs of the anatase-type phases prepared at 650°C showed weight increases, beginning at 250°C and completed at 650°C, agreeing with the oxidation reaction $Ti_xTa_{1-x}O_{1+x}N_{1-x} \rightarrow Ti_xTa_{1-x}O_{2.5-0.5x} + (1-x)/2N_2$. Samples prepared at 600°C showed, however, *ca* 25% smaller weight increases, possibly because they were not completely converted to the anatase phase by the ammonolysis, and therefore contain an amorphous phase with a smaller nitrogen content.

One of the samples ($x = 0.68$, ammonolysed at 650°C) was selected for further characterisations. The O and N contents were determined by the combustion method. Given the nominal Ti:Ta ratio, the results of the analysis were consistent with the composition $Ti_{0.68}Ta_{0.32}O_{1.68(1)}N_{0.32(1)}$. A Rietveld refinement of the structure was carried out, using X-ray CuK$\alpha_1$ diffractometer data, with a total of 12 parameters and 20 theoretical Bragg

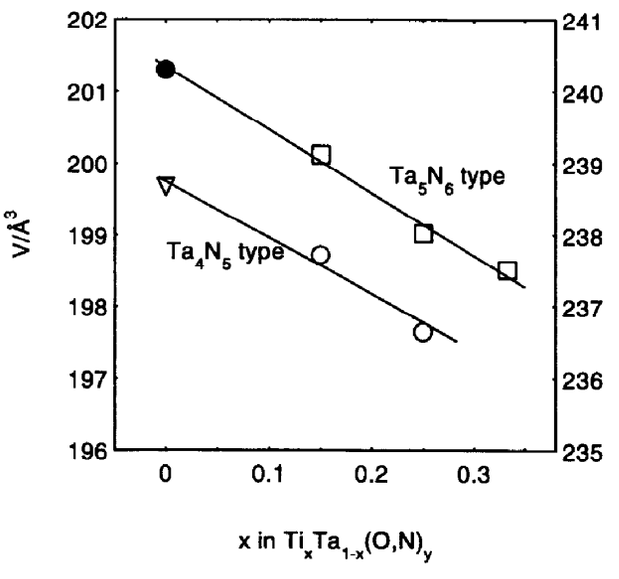


**Fig. 2.** Unit-cell volumes of the $Ta_4N_5$-type phase (○) and the $Ta_5N_6$-type phase (□) versus x in $Ti_xTa_{1-x}$; $Ta_4N_5$[1] (▽); $Ta_5N_6$[1] (●).

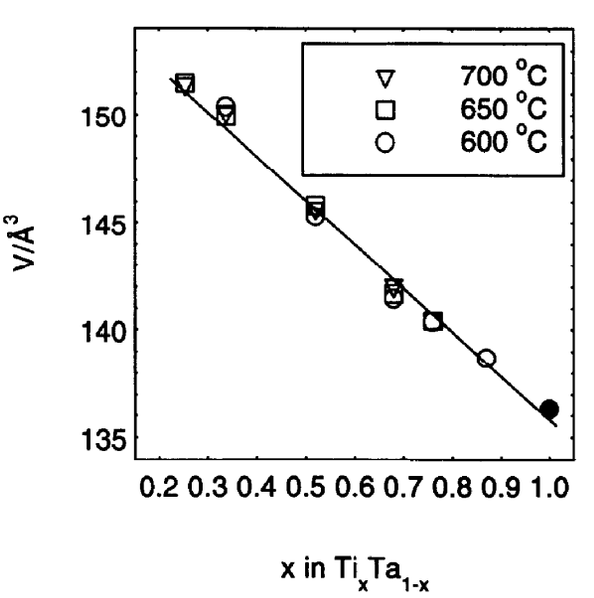


**Fig. 3.** Unit-cell volumes of anatase-type $Ti_xTa_{1-x}O_{1+x}N_{1-x}$ versus x in $Ti_xTa_{1-x}$; $TiO_2$[6] (●).

reflections for $2\theta < 83°$. A collective temperature factor was used for the (Ti,Ta) and (O,N) atoms. The half-width of the peaks was 0·50 in $2\theta$ at $2\theta = 47°$. The refinement yielded $R_F = 3{\cdot}0\%$ and $S = 1{\cdot}4$. Figure 4 shows the fit between the calculated and observed patterns. A list of atomic co-ordinates and distances is given in Table 1, with the esd:s multiplied by 3·9 in order to account for serial correlation.[10] The refinement confirms that the oxynitride phases $Ti_xTa_{1-x}O_{1+x}N_{1-x}$, $0{\cdot}52 \leq x \leq 0{\cdot}87$, are isostructural with anatase.

The electrical conductivity of a pressed rod of $Ti_{0{\cdot}68}Ta_{0{\cdot}32}O_{1{\cdot}68}N_{0{\cdot}32}$ was measured between 186 and 406 K, by the 4-probe method. The conductivity at room temperature was determined to *ca* $4{\cdot}10^{-5}\,\Omega^{-1}{\cdot}m^{-1}$. The temperature variation of the conductivity could be described accurately by an expression for two thermally activated conduction mechanisms in parallel: $\sigma = \sigma_{0A}\exp(-E_A/kT) + \sigma_{0B}\exp(-E_B/kT)$, with $\sigma_{0A} = 0{\cdot}20\,\Omega^{-1}{\cdot}m^{-1}$, $E_A = 0{\cdot}238$ eV and $\sigma_{0B} = 9{\cdot}6{\cdot}10^{-5}\,\Omega^{-1}{\cdot}m^{-1}$, $E_B = 0{\cdot}036$ eV. The two conductivity components may correspond to a a bulk conductivity and a conduction via grain boundaries. Magnetic susceptibility measurements for $Ti_{0{\cdot}68}Ta_{0{\cdot}32}O_{1{\cdot}68}N_{0{\cdot}32}$ showed a temperature-independent paramagnetic suceptibility of $2{\cdot}2{\cdot}10^{-9}$ $m^3{\cdot}mol^{-1}$ for T = 70–320 K. At lower temperatures, the magnetic susceptibility increased with decreasing temperature, possibly due to paramagnetic impurities, reaching $3{\cdot}8{\cdot}10^{-9}\,m^3{\cdot}mol^{-1}$ at 11 K.

### 3.3 Cubic NaCl-type phases

A cubic phase was obtained for all compositions at 900°C. X-ray pure samples were obtained for $0{\cdot}52 \leq x \leq 1$, while preparations with lower x values also contained the $Ta_3N_5$-type phase. The amount of cubic phase decreased at lower temperatures, accompanied by increasing amounts of $Ta_3N_5$-, TaON- and anatase-type phases, and at higher temperatures by $Ta_4N_5$- and $Ta_5N_6$-type phases. The cubic phase was obtained for x = 1 at all temperatures studied. The colour of the phase was black, except for x = 1 prepared at 900–1000°C, which was brown. The XRPD patterns of the phase could be indexed with a face-centered unit cell with *a* ranging between 4·2 and 4·3 Å. Cell constants for the cubic phases, obtained at different temperatures and compositions, are shown in Fig. 5 together with reported unit cell volumes for TiO (JCPDS No. 8-117) and TiN (JCPDS No. 38-1420). The cell constant is expected to decrease with increasing Ti content and number of possible vacancies on cation sites, and to increase with the N/O ratio. The increase of the cell constants with preparation temperature can thus be ascribed to an increase in the N/O ratio and/or a decrease of cation vacancy content. The comparatively constant *a* values for $x < 0{\cdot}52$ at 1000°C may be connected with a Ti enrichment of the cubic phase.

The X-ray monophasic cubic phases were oxidised in the TG unit. The measurements made

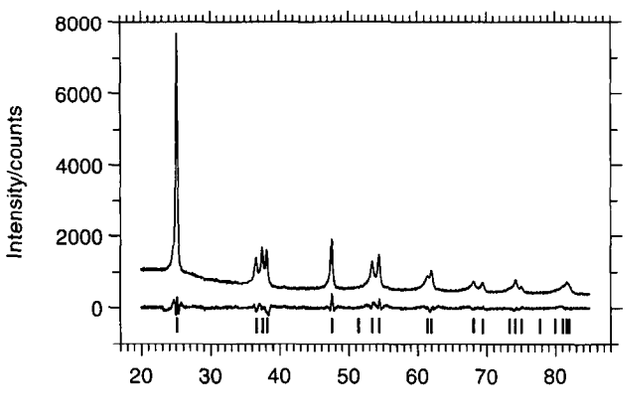


**Fig. 4.** Observed and difference intensity X-ray patterns of $Ti_{0{\cdot}68}Ta_{0{\cdot}32}O_{1{\cdot}68}N_{0{\cdot}32}$.

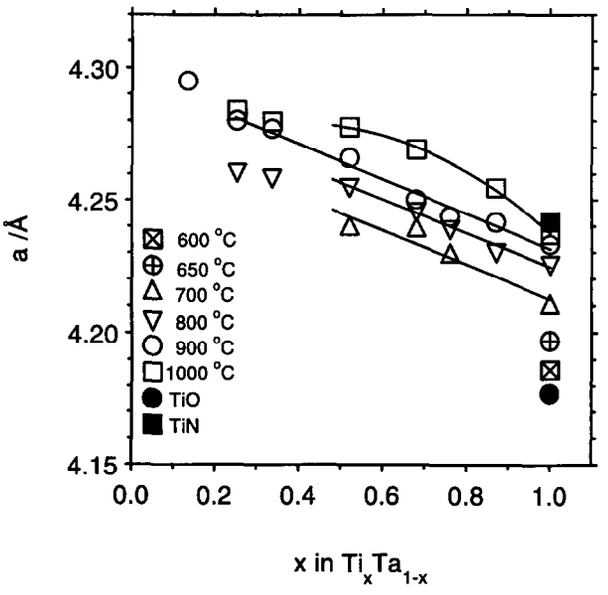


**Fig. 5.** Cell constants *a*(Å) of cubic (oxy)nitride (Ti,Ta)(O,N)$_y$ phases versus x in $Ti_xTa_{1-x}$; TiO (●), TiN (■).

**Table 1.** Atomic co-ordinates and bond distances (Å) for anatase-type $Ti_{0{\cdot}68}Ta_{0{\cdot}32}O_{1{\cdot}68}N_{0{\cdot}32}$; space group $I4_1/amd$; $a = 3{\cdot}838(1)$, $c = 9{\cdot}618(5)$ Å and Z = 4

| *Atom* | *Site* | *x* | *y* | *z* | *B*/Å$^2$ |
|---|---|---|---|---|---|
| Ti,Ta | 4*a* | 0 | 1/4 | 7/8 | 0·9(1) |
| O,N | 8*e* | 0 | 1/4 | 0·085(2) | 0·9(1) |
| Ti,Ta- | O,N | 4x1·958(4) | | | |
| | O,N | 2x2·02(2) | | | |
| Mean | | 1·98 | | | |

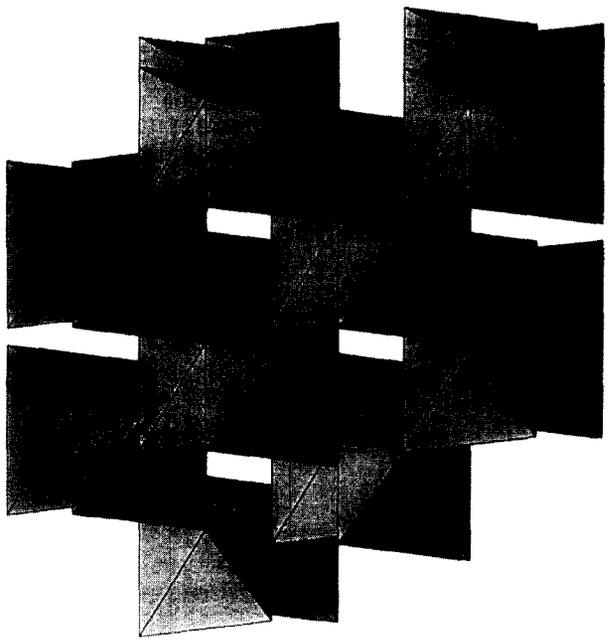

**Fig. 6.** A polyhedral illustration of the anatase structure.

some deductions possible, although the determined weight increase by itself is insufficient to determine the composition, since the oxidation states of the metal atoms in the cubic phases are not known. The weight increase began at *ca* 250°C for samples prepared at 650–800°C, and was completed at *ca* 500°C. For samples ammonolysed at 900–1000°C, the weight increase commenced at higher temperatures, *ca* 400–500°C and a constant-weight plateau was not reached below 1000°C for $x = 0.87$. The weight gain increased substantially with the sample preparation temperature, implying a higher nitrogen and/or less cation vacancy content in samples ammonolysed at higher temperatures. Furthermore, the observed weight increases were too small in general to correspond to an oxidation of either $MN$ or $MO$, $M$=(Ti,Ta) compositions (assuming the end products to be oxides containing $Ti^{4+}$ and $Ta^{5+}$), implying the presence of cation vacancies. For $x = 1$ the data are consistent with e.g. compositions $Ti_{0.82}O$ or $Ti_{0.72}N$ for the 650°C preparation and e.g. $TiN_{0.58}O_{0.42}$ and $Ti_{0.94}N$ for the samples prepared at 900 and 1000°C.

## 4 Discussion and Conclusions

A polyhedral illustration of the anatase ($TiO_2$) structure[6,7] is shown in Fig. 6. The oxygen atoms form a distorted cubic close-packed array and the structure contains zig-zag chains of edge-sharing $TiO_6$ octahedra. Each $TiO_6$ octahedron shares four edges. Two Ti-O distances (along the *c* axis) are longer than the other four. Isostructural compounds are $Ti_{0.85}Sn_{0.15}O_2$[11] and TiNF.[12] Compounds isostructural with $\alpha$-$LiFeO_2$[13,14] can be regarded as 'stuffed' derivates of the anatase-type structure. The idealised, ordered, structure of $\delta'$-$Ti_2N$[15] is an anti-anatase type.

The present study, as well as the previous investigation of phase formation in the $Zr_xTa_{1-x}(O,N)_y$ system, shows that solid solution phases can be prepared that exhibit the substitution mechanism $M^{4+} + O^{2-} \leftrightarrow Ta^{5+} + N^{3-}$ with $M$ = Ti and Zr. The stability of the phases is partly connected with the strong ability of Ta to retain the oxidation state of +5 in (oxy)nitrides. In order to prepare the phases, it is very likely crucial that homogeneous starting materials are used for the ammonolysis, e.g. gels, since the phases form at comparatively low temperatures.

## Acknowledgements

I wish to thank Dr T. Hörlin for the conductivity measurement, and my co-workers in this project, Drs P-O. Käll and G. Svensson, and also Prof. M. Nygren for support and valuable discussions.

## References

1. Grins, J., Käll, P.-O. and Svensson, G., Phases in the $Zr_xTa_{1-x}(O,N)_y$ system, formed by ammonolysis of Zr-Ta gels: preparation of a baddeleyite-type solid solution phase $Zr_xTa_{1-x}O_{1+x}N_{1-x}0 \leq x \leq 1$. *Journal of Mater. Chem.*, 1994, **4**(8), 1293–1301.
2. Landolt-Börnstein, ed. Hellwege, K. H. and Hellwege, A. M., Series III Vol. 7c, Springer-Verlag, Berlin/Heidelberg, 1978.
3. Collongues, R., Gilles, J.-C. and Lejus, A.-M., Action de l'ammoniac sur différents oxydes super-réfractaires. *Bull. Soc. Chim. Fr.*, 1962, 2113–2117.
4. Wiles, D. B., Sakthivel, A. and Young, R. A., *Users Guide to Program DBW3.2S for Rietveld Analysis of X-ray and Neutron Powder Diffraction Data Patterns (Version 8804)*. School of Physics, Georgia Institute of Technology, Atlanta, 1985.
5. Fontbonne, A. and Gilles, J.-C., Noveaux nitrures de tantale. Nitrure et oxynitrures mixtes de tantale et de niobium. *Rev. Int. Hautes Tempér. et Réfract.*, 1969, **6**, 181–192.
6. Howard, C. J., Sabine, T. M. and Dickson, F., Structural and thermal parameters for rutile and anatase. *Acta Cryst.*, 1991, **B47**, 462–468.
7. Burdett, J. K., Hughbanks, T., Miller, G. J., Richardson Jr., J. W. and Smith, J. V., Structural-electronic relationships in inorganic solids: powder neutron diffraction studies of the rutile and anatase polymorphs of titanium dioxide at 15 and 295 K. *Journal of Am. Chem. Soc.*, 1987, **109**, 3639–3646.
8. Weishaupt, M. and Strähle, J., Darstellung der oxidnitride VON, NbON und TaON. Die Kristallstruktur von NbON und TaON. *Z. Anorg. Allg. Chem.*, 1977, **429**, 261–269.
9. Brese, N. E., O'Keffe, M., Rauch, P. and DiSalvo, F. J., Structure of $Ta_3N_5$ at 16 K by time-of-flight neutron diffraction. *Acta. Cryst.*, 1991, **C47**, 2291–2294.
10. Bérar, J.-F. and Lelann, P., E.S.D.'s and estimated probable error obtained in Rietveld refinements with local correlations. *Journal of Appl. Crystallogr.*, 1991, **24**, 1–5.

11. Yamane, H., Young, B. C. and Hirai, T., Crystal structure of anatase-type $TiO_2$-$SnO_2$ solid solution prepared by CVD. *Journal of Ceram. Soc. Jpn.*, 1992, **100**, 1473–1474.
12. Wüstefeld, C., Vogt, T., Löchner, U., Strähle, J. and Fuess, H., Synthesis of TiNF and structure determination by powder diffraction using synchrotron radiation. *Angew. Chem. Int. Ed. Engl.*, 1988, **27**, 929–930.
13. Hoffman, L. and Hoppe, R., Zur Kenntnis des $\alpha$-$LiFeO_2$-typs. Z. *Anorg. Allg. Chem.*, 1977, **430**, 115–120.
14. Kuo, Y. B., Scheld, W. and Hoppe, R., To the knowledge of the $\alpha$-$LiFeO_2$ type: an examination of $LiScO_2$ and $NaNdO_2$. *Z. Kristallogr.*, 1983, **164**, 121–127.
15. Christensen, A. N., Alamo, A. and Landesman, J. P., Structure of vacancy-ordered titanium heminitride $\beta'$-$Ti_2N$ by powder neutron diffraction. *Acta Cryst.*, 1985, **C41**, 1009–1011.